JOURNAL OF AIRCRAFT
Vol. 45, No. 2, March–April 2008

Characterization of In-Plane Shear Properties of Laminated Composites at Medium Strain Rates

K. S. Raju* and S. Dandayudhapani†
Wichita State University, Wichita, Kansas 67260-0044
and
C. K. Thorbole‡
The Engineering Institute, Farmington, Arkansas 72730

DOI: 10.2514/1.30026

The in-plane shear responses of continuous fiber reinforced composite materials under medium strain rates have been characterized experimentally. The V-notch rail shear apparatus was used for characterizing the in-plane shear behavior of Newport NB321/3k70 plain weave carbon fabric/epoxy and NB321/7781 fiberglass/epoxy systems. The testing was conducted using a high-rate servo-hydraulic testing machine at nominal stroke rates ranging between 2.5×10^{-5} and 2.54 m/s. A maximum estimated shear strain rate of 200 rad/s was achieved up to shear strain levels of 0.08 rad during the tests. The shape of the stress-strain curves at stroke rates up to 0.254 m/s were similar, with the stress levels increasing with the stroke rate at a given strain level. However, at a stroke rate of 2.54 m/s, the stress-strain behavior changed drastically indicating wave propagation effects. No change in failure modes was observed for the range of test speeds investigated.

I. Introduction

THE use of composite materials for structural applications has many advantages, which include higher specific strength and stiffness, better durability, etc. [1]. The widespread use of composite materials in airframe structures coupled with the crashworthiness requirements have necessitated the material characterization at high strain rates. The crashworthiness of composite airframe structures has typically been addressed using drop tests on full-scale and/or scaled test articles [2–4]. The full-scale tests have indicated that energy absorption in composite structures is through tailored failure mechanisms rather than plastic deformations prevalent in metallic structures. The test results are useful in the appraisal of the performance of the structure and any energy absorption devices under crash loading, but do not reveal the various mechanisms that do and do not contribute to the overall performance of the structure. Further, the performances of individual components may be influenced by the overall structural assembly. To investigate the effectiveness of various components, numerical modeling would be more appropriate and less expensive. However, the predictions of the numerical models are dependent on the geometric definition of the structure, the material models, failure criteria, etc. Several investigations have simulated the experiments numerically albeit using quasi-static test data. The simulations include simple energy absorption devices, fuselage assemblies, etc. The predictions based on quasi-static material properties have resulted in significant deviations from test data. The description of material behavior under dynamic loading is thus an important aspect of the numerical modeling of dynamic loading scenarios.

The dynamic characterization of composite material properties has typically been conducted using electromechanical and servo-hydraulic machines, split Hopkinson pressure bar (SHPB) apparatus [5], etc. The constant rate testing machines have been employed for strain rates approaching 100 s^{-1}, whereas the SHPB apparatus is used for strain rates exceeding 1000 s^{-1}. The properties that have been characterized by the past researchers include the tensile and compressive properties (both in plane and transverse) and interlaminar shear properties [6–9].

The in-plane shear characterization of laminated composites has been accomplished using different methods under quasi-static loading [1]. The popular methods are the Iosipescu method, the off-axis tension tests, three-rail shear, torsion, modified V-notch rail shear, picture-frame test, etc. In these tests, the shear strains are obtained by the measurement of normal strains along two orthogonal directions and the use of strain transformation equations [1]. The off-axis tests capture the linear portion of the shear stress–shear strain behavior, but the ultimate strength data are not accurate. This is due to the large deformations associated with off-axis tests, which result in a change of fiber orientations and the failure initiation being dominated by edge effects. The in-plane shear characterization under high-rate loading has typically been addressed using an off-axis specimen [9]. The off-axis specimens have been loaded under tension or compression using SHPB apparatus to study the effects of strain rate on the strength of the material. Because of the small specimen size used in the SHPB tests, the measurement of strains along two orthogonal directions may not be practical, resulting in the characterization of shear strength alone. Staab and Gilat [10] reported that the off-axis specimen strengths were more sensitive to strain rate for shallower fiber angles, indicating that the fibers were more rate sensitive than the matrix. Hallett et al. [11] used a single-lap shear specimen to characterize the interlaminar shear properties of carbon/epoxy cross-ply laminates. The specimens were tested using SHPB apparatus and the shear strains were measured using miniature gauges with a gauge length of 1 mm bonded to the specimen. The in-plane shear characterization of fabric reinforced laminates will require a larger gauge area and strain gauges that encompass at least a few unit cells. Thus, in this investigation the in-plane shear characterization was done using the modified V-notch rail shear method [12].

The high-rate characterization using a servo-hydraulic machine is typically conducted under the tension loading mode, in which the actuator is moving away from a fixed crosshead. This mode of testing

Presented as Paper 2258 at the 47th AIAA/ASME/ASCE/AHS/ASC Structures, Structural Dynamics, and Materials Conference, Newport, Rhode Island, 1–4 May 2006; received 25 January 2007; revision received 27 April 2007; accepted for publication 5 June 2007.

*Assistant Professor, Department of Aerospace Engineering, Box 44. Professional Member AIAA.
†Graduate Student, Department of Aerospace Engineering, Box 44.
‡Chief Research Engineer, Occupant Safety, Post Office Box 610, 13045 West Highway 62.

is preferred over compression loading, unless the specimen accommodates an appreciable amount of deformation, allowing for the actuator to decelerate post specimen failure. In this investigation, the modified V-notch rail shear method was preferred over the Iosipescu method for characterization of the in-plane shear behavior, primarily due to the tensile mode of loading required to shear the specimen. Because the test fixture halves move away from each other, there is no danger of them running into each other during high-speed testing. The modified V-notch rail shear method offers several advantages, which include higher load and deformation capability and larger gauge regions. However, owing to the mass of the fixtures, the inertial effects may influence the load measurement and validity of the test at higher speeds.

In this investigation, the in-plane shear responses of two material systems sharing the same matrix but different reinforcement types have been studied experimentally. The objective of the investigation was to generate shear stress-strain curves at different strain rates and study the effects of strain rate on the in-plane shear strengths and failure modes of the two material systems. The details of the experimental apparatus, results and observations, and limitations of the current approach are reported in this paper.

II. Material Systems and Test Apparatus

The material systems used in the current investigation were the Newport NB321/3k70 plain weave carbon fabric/epoxy prepreg (PWCF) system and the NB321/7781 fiberglass/epoxy prepreg (SWGF) system. Both material systems share the same resin system with a nominal cure temperature of 135°C. The nominal mechanical properties of the two material systems are summarized in Table 1. Flat laminates measuring 1.2 m × 0.3 m, with a stacking sequence of $[0]_{12}$, were fabricated and cured using an autoclave cure cycle. The laminates were subsequently cut into V-notch specimens per ASTM D7078 [12]. The typical test specimen geometry is illustrated in Fig. 1. The PWCF test specimens had a nominal thickness of 2.72 mm, whereas the SWGF specimens had a nominal thickness of 3.30 mm.

The pertinent dimensions [12] of the test specimens were measured and recorded before the bonding of strain gauges to the specimens. Vishay Micro-Measurements[§] EA125TH-120, ±45° strain rosettes were bonded at the center of the gauge section to measure the shear strains during the test. The strain gauge is capable of measuring an apparent maximum shear strain of 0.1 rad. It should be noted that the shear strain at failure for most materials exceeds this value. The test specimens were tested at room temperature (23°C, 35% relative humidity), at different stroke rates, using an MTS[¶] high-rate servo-hydraulic testing machine. The testing machine has a stroke range of 0.38 m and can reach speeds up to 12.7 m/s. The load capacity (sustained) of the machine is 22 kN at rated speed and 39 kN at speeds lower than 1 m/s. The force measurement was accomplished using a PCB Peizolectronics[**] 206C ICP® quartz force ring that was calibrated to measure ±44 kN with an upper frequency limit of 40 kHz. The strain gauge signals were conditioned using Vishay Micro-Measurements model 2100 strain gauge signal conditioners. An excitation voltage of 10 V was used to maximize the available bandwidth of the signal conditioner. The higher excitation voltage tended to heat the specimen by about 10°C. The temperature was monitored and allowed to stabilize before the test. The data acquisition was accomplished using National Instruments[††] PCI-6111 simultaneous sampling data acquisition board. The data was acquired with a 12 bit resolution and data acquisition rates up to 5 MHz. The load, actuator displacement, and strain readings were recorded during the tests.

The shear test fixture consists of two halves, one of which was fastened to the load cell while the other was fastened to the actuator as illustrated in Fig. 2. The high-rate testing machine requires a finite stroke length to accelerate to the desired speed. A stroke length of 0.065 m is traversed by the actuator before reaching a speed of 12.7 m/s. This length of stroke, during which the acceleration takes place, decreases with the final speed to be attained. The typical stroke length required to fail a composite specimen in shear is about 8 mm, which is very small in comparison to that of the acceleration phase. Thus, the specimen (or fixture) must be engaged by the specimen after the desired speed has been achieved. To accomplish this, a *slack-inducer* mechanism was designed and fabricated. The mechanism consists of a slotted tube that is fastened to the actuator. A slack rod rides inside the slack tube and the free end of this rod is connected to the fixture. A pin passing through the slack rod slides in a slot provided in the tube. When the pin reaches the end of the slot, the specimen is engaged and load-transfer occurs. The schematic of the slack-inducer mechanism is illustrated in Fig. 2. Even though the slack-inducer mechanism helps engage the specimen after the actuator has reached the desired speed, a constant stroke rate test is not guaranteed owing to the flexibility of the various components forming the slack-inducer mechanism.

Table 1 Nominal quasi-static mechanical properties of the material systems [13]

Material system	NB321/3k70 PWCF	NB321/7781 SWGF
Nominal fiber volume fraction v_f	0.55	0.57
Nominal ply thickness t_{PLY}, mm	0.216	0.27
In-plane modulus $E_L = E_T$, GPa	66.1	27.9
In-plane shear modulus G_{LT}, GPa	4.2	4.2
In-plane tensile strength F^{TU}, MPa	620	438
In-plane compressive strength F^{CU}, MPa	477	537
In-plane shear strength F_{12}^{SU}, MPa	114.8	130

III. Experimental Results

The shear testing was conducted at nominal stroke rates of 2.1×10^{-5}, 0.0254, 0.254, and 2.54 m/s. Three replicates were tested at each of the aforementioned speeds. The recorded test data were reduced to obtain time histories of stress, shear strain, and stress-strain curves for each specimen. The specimens were examined posttest to study the effects of test speed on the failure modes.

The strain time history from a test conducted at a quasi-static stroke rate is shown in Fig. 3. Because the test was conducted at a constant stroke rate, the strain rate was not uniform throughout the test. Based on the strain gauge signal, it can be inferred that the shear strain rate varies linearly with time, at least up to the shear strain value of 0.08 rad. A constant shear strain rate could be conducted by using the strain signal as a feedback, but will be limited by the maximum strain that can be measured by strain gauges. Further, the constant

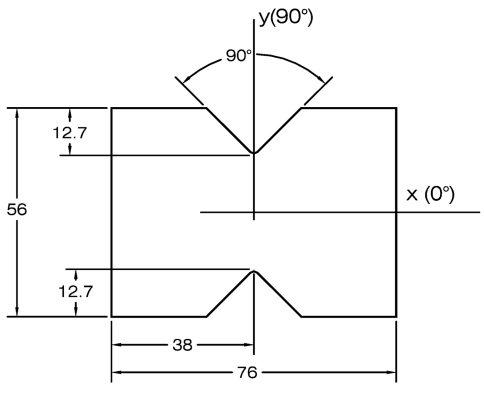

Fig. 1 Test specimen geometry [12].

[§]Vishay Micro-Measurements, P. O. Box 27777, Raleigh, NC 27611

[¶]MTS Corporation, Eden Prairie, MN

[**]PCB Piezotronics, Inc., 3425 Walden Avenue, Depew, NY 14043-9902

[††]National Instruments Corporation, 11500 N Mopac Expwy, Austin, TX 78759-3504

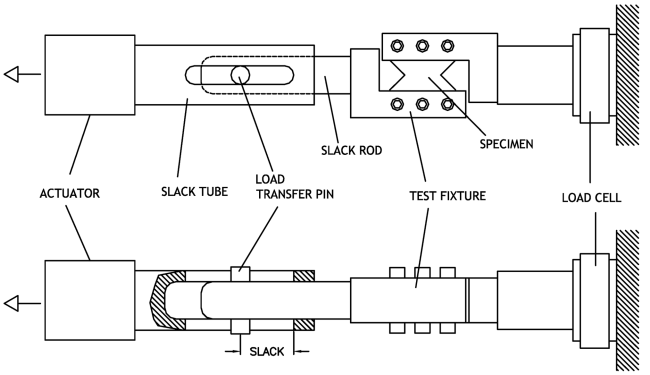

Fig. 2 Test apparatus for high-rate testing.

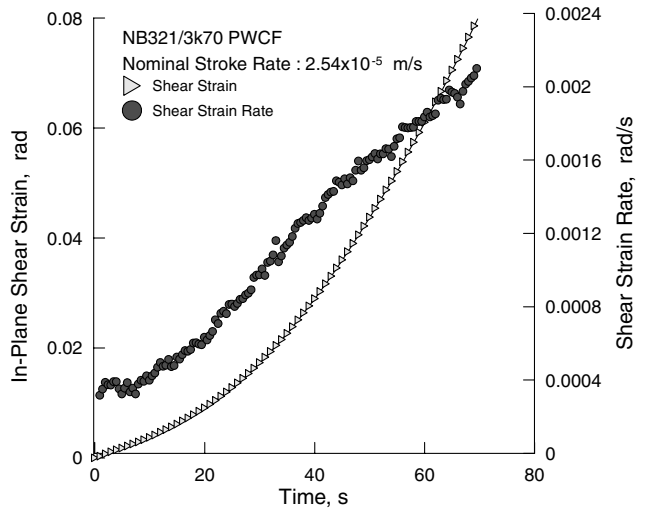

Fig. 3 Shear strain and shear strain-rate history from a quasi-static test.

strain-rate test will require the actuator to decelerate to compensate for the increasing strain rate, which would be difficult to achieve at higher stroke rates. Further, the flexibility of elements forming the load train between the specimen and the actuator contribute to the nonuniformity of the stroke rate at the specimen fixture. Thus, in this investigation, the term *constant stroke rate* refers to the actuator speed and not the relative displacement between the fixture halves. The variation of shear strain for tests conducted at different stroke

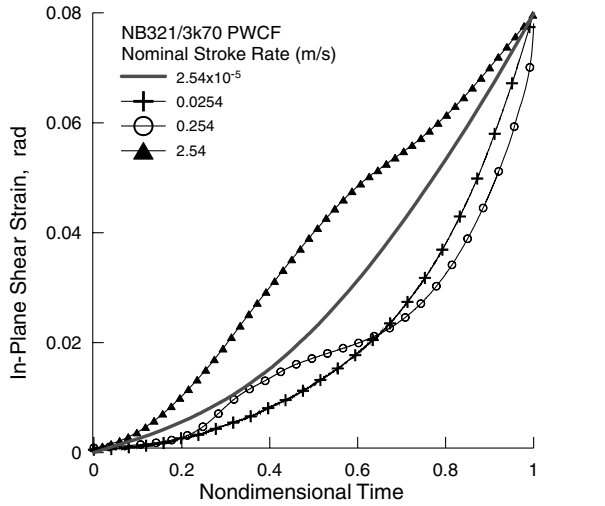

Fig. 4 Time history of a shear strain for tests conducted at different stroke rates.

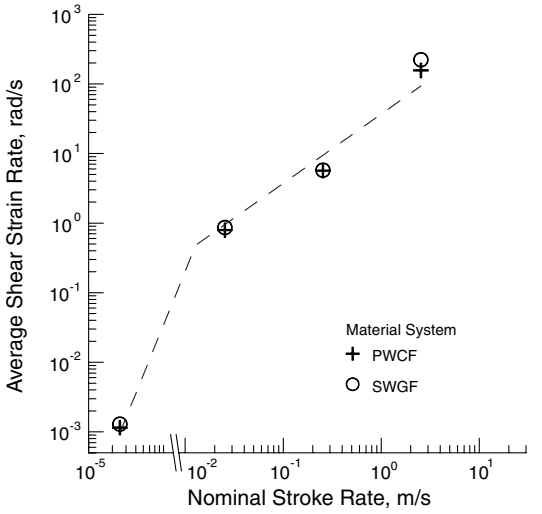

Fig. 5 Average strain rates achieved at different stroke rates up to a maximum strain level of 0.08 rad.

rates is summarized in Fig. 4. The shear strain is plotted against a nondimensional time to enable comparison between tests conducted at different stroke rates. The time was normalized by the time required to attain a shear strain level of 0.08 rad. It can be observed from the figure that the shear strain histories are similar for tests conducted at stroke rates of 2.54×10^{-4}, 0.0254, and 0.254 m/s. However, the variation of the strain at a stroke rate of 2.54 m/s is significantly different and attributed to the dynamics of the slack-inducer mechanism. An average strain rate was computed for each test up to a maximum shear strain value of 0.08 rad. The variation of the average shear strain rate as a function of stroke rate is presented in Fig. 5. In the current study, average strain rates ranging between 10^{-3} to 200 rad/s were attained over a shear strain range of 0.08 rad, for both the material systems tested.

A. Stress-Strain Characterization

The typical shear stress versus actuator displacement and shear stress-strain diagrams obtained from the tests conducted at quasi-static rates for the two material systems investigated are illustrated in Figs. 6a and 6b. Both materials exhibit identical behavior as seen in the two figures, with the PWCF material exhibiting slightly higher stresses in the nonlinear region. The stress-strain diagram is truncated at a shear strain value of 0.1 rad, which is the limit of the strain gauge. The test specimens can sustain a load beyond this strain limit as seen in the stress versus actuator displacement diagram. It should be noted that the shear strains are obtained from normal strains measured along two orthogonal directions, using transformation equations based on small-strain theory. Owing to small normal strains along the length of the specimen (x direction) due to constraint effects, and assuming uniform shear strain distribution over the area covered by the strain gauge, the error will be less than 0.5%.

The time histories of shear strain and stress (or load) for a test conducted at a stroke rate of 2.54 m/s is illustrated in Fig. 7. Because the strain measurement occurs directly, it leads the load signal in phase. The load signal is modulated in phase and amplitude due to the load path in between the test fixture and the load cell and wave propagation effects in the specimen. For the experimental setup used in the current study, the phase difference was observed to be negligible for stroke rates of 0.254 m/s and below. To plot the stress-strain curves, the load (or strain) signal was shifted in time. The load signal must be further corrected for amplitude modulation using an appropriate system transfer function, which is a part of ongoing work. The results presented in this paper, however, do not incorporate any corrections to the load signal.

The shear stress-strain behavior of SWGF and PWCF materials recorded at tests conducted at different stroke rates is illustrated in

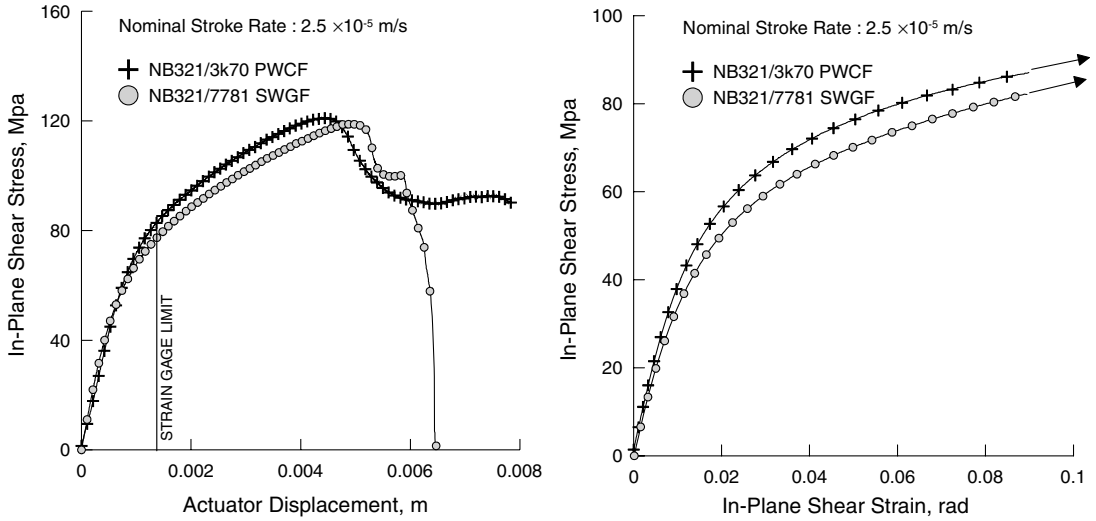

Fig. 6 Diagrams for PWCF and SWGF material tested at quasi-static test rate: a) shear stress versus actuator displacement, and b) Shear stress–shear strain.

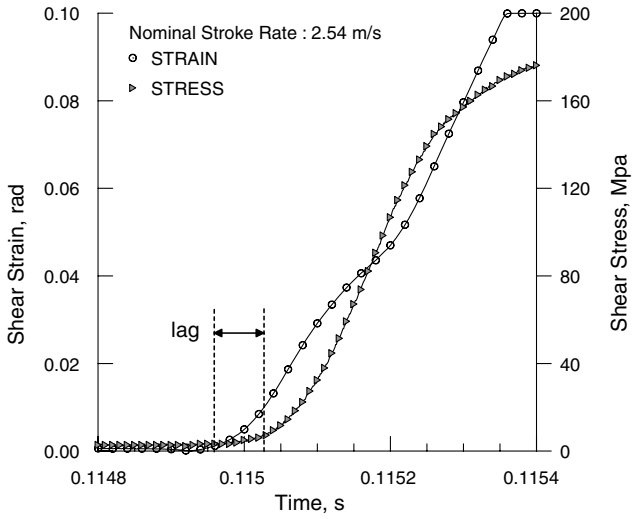

Fig. 7 Phase difference between strain and load signal during a high-speed test.

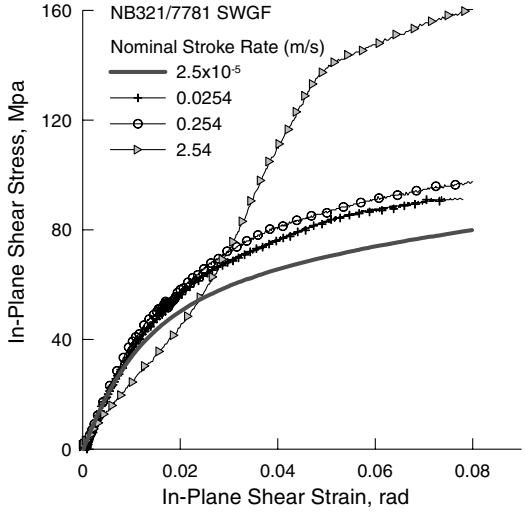

Fig. 8 Stress–strain plots for SWGF material tested at different stroke rates.

Figs. 8 and 9, respectively. The shapes of the stress-strain curves are similar to that of the quasi-static test, up to a stroke rate of 0.254 m/s for both materials. At any strain level, the shear stress levels increase with stroke rate for both materials, with the SWGF material being slightly more rate sensitive. At stroke rates of 2.54 m/s, the stress-strain behavior appears to change significantly, with an appreciable decrease in material stiffness. The distortion of the stress-strain curves at this speed could be due to the load signal modulation, wave propagation effect, and/or change in material behavior, and must be further investigated. The in-plane shear-strengths of PWCF and SWGF materials are plotted as a function of nominal stroke rate in Fig. 10. The in-plane shear strengths increase with stroke rate, with little difference between the two material systems. This indicates that the strain-rate sensitivity is independent of the reinforcement type.

The strain rate sensitivity of the material shear stress strain behavior may be captured using a hyperbolic function [14] based power law given in Eq. (1).

$$\tau = \tau_U \tanh\left(\frac{G_{\mathrm{LT}}}{\tau_U}\gamma\right)\left(\frac{\dot{\gamma}}{\dot{\gamma}_{\mathrm{REF}}}\right)^n \tag{1}$$

The shear strength, τ_U, and shear modulus, G_{LT}, at a nominal shear strain rate, $\dot{\gamma}_{\mathrm{REF}}$, may be obtained by conducting a strain-controlled

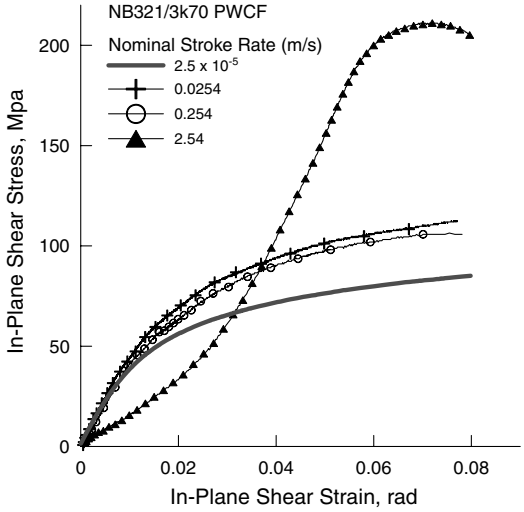

Fig. 9 Stress–strain plots for PWCF material tested at different stroke rates.

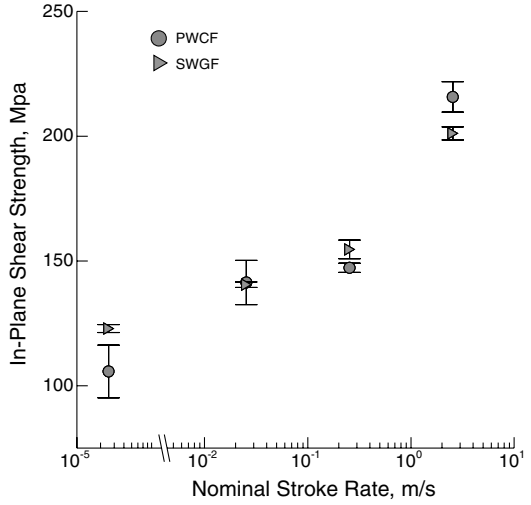

Fig. 10 In-plane shear strength as a function of stroke rate for PWCF and SWGF materials.

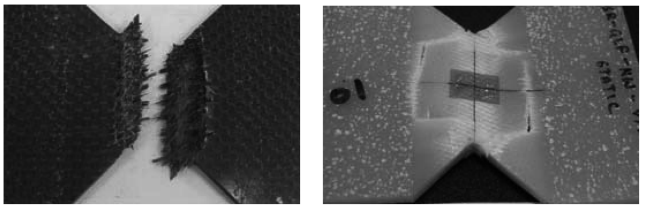

Fig. 11 Typical failure modes in PWCF (left) and SWGF (right) specimens tested at different test speeds.

quasi-static test. However, the determination of the rate sensitivity exponent, n, may not be straightforward owing to the variation of the shear strain rate, $\dot{\gamma}$, throughout the test. Further, the equation assumes that the rate effects are independent of the magnitude of the shear strain.

B. Failure Modes

The failure modes in the test specimens were examined posttest to investigate the influence of strain rate. The failure modes in PWCF specimens tested at rates up to 0.254 m/s were primarily shear failure across the minimum cross section. The shear failure occurs over a narrow band between the notches. The failure surface tends to be oriented at a shallow angle to the plane of the specimen, with fractured fibers protruding out of the surface. The failure modes for SWGF specimens tended to follow the same trends as the PWCF material. However, a large band of process zone was visible due to the translucency of the material, as illustrated in Fig. 11. The width of this band was observed to increase with the loading rate. The fracture planes for SWGF specimens were located away from the minimum section at all loading rates. To enforce failure across the minimum section at higher rates, a deeper notch may have to be used.

IV. Conclusions

The effects of strain rate on the in-plane shear behavior of Newport NB321/3K70 PWCF and NB321/7781 SWGF material systems were investigated experimentally. The testing was conducted using a servo-hydraulic testing machine at nominal stroke rates ranging between 2.5×10^{-5} and 2.54 m/s. A maximum estimated shear strain rate of 200 rad/s was achieved up to shear strain levels of 0.08 rad during the tests. The stress-strain behavior of both material systems exhibited similar behavior with increasing stroke rates up to 0.254 m/s. The stress-strain curves exhibited an asymptotic behavior for stroke rates approaching 0.254 m/s and were dependent on the material systems at a stroke rate of 2.54 m/s. The shear strengths exhibited an increasing trend with the stroke rate. At the highest test rate, the shear strengths increased by a factor of 2 relative to that of the quasi-static rates and were independent of the reinforcement type.

Acknowledgments

The authors would like to thank J. Zvanya, Program Monitor, FAA William J. Hughes Technical Center, Atlantic City, NJ, for his support and encouragement. The authors express their gratitude to J. S. Tomblin, Executive Director, National Institute for Aviation Research, for making the resources available to successfully complete this work.

References

[1] Daniel, I.M., and Ishai, O., *Engineering Mechanics of Composites*, Oxford Univ. Press, New York, 1994.

[2] Farley, G. L., "Energy Absorption Capability and Scalability of Square Cross-Section Tube Specimens," *Journal of the American Helicopter Society*, Vol. 34, April 1989, pp. 59–62.

[3] Carden, H. D., and Hayduk, R. J., "Airplane Subfloor Response to Crash Loadings," Society of Automotive Engineers Technical Paper 810614, 1981.

[4] Farley, G. L., "Crash Energy Absorbing Sub-Floor Beam Structures," *Journal of the American Helicopter Society*, Vol. 32, Oct. 1987, pp. 28–38.

[5] Kolsky, H., " An Investigation of the Mechanical Properties of Materials at Very High Rates of Loading," *Proceedings of the Royal Society of London, Series A: Mathematical and Physical Sciences*, No. B62, 1949, pp. 676–700.

[6] Hayes, S. V., and Adams, D. F., "Rate Sensitive Tensile Impact Properties of Fully and Partially Loaded Unidirectional Composites," *Journal of Testing and Evaluation*, Vol. 10, No. 2, 1982, pp. 61–68.

[7] Daniel, I. M., and Liiber, T., "Testing Fiber Composites at High Strain Rates," *Proceedings of the 2nd International Conference on Composite Materials*, ICCM, Toronto, 1978, pp. 1003–1018.

[8] Peterson, B. L, Pangborn, R. N, and Pantano, C. G., "Static and High Strain Rate Response of a Glass Fiber Reinforced Thermoplastic," *Journal of Composite Materials*, Vol. 25, July 1991, pp. 887–906.

[9] Tsai, J., and Sun, C. T., "Strain Rate Effect on Dynamic Compressive Failures in Off-Axis Glass-Epoxy Composites," *Dynamic Failure in Composite Materials and Structures*, Vol. 243, American Society of Mechanical Engineers, New York, 2000, pp. 13–24.

[10] Staab, G. H., and Gilat, A., "High Strain Rate Response of Angle-Ply Glass/Epoxy Laminates," *Journal of Composite Materials*, Vol. 29, No. 10, 1995, pp. 1308–1320.

[11] Hallett, S. R., Ruiz, C., and Harding, J., "The Effect of Strain Rate on the Interlaminar Shear Strength of a Carbon/Epoxy Cross-Ply Laminate: Comparison Between Experiment and Numerical Prediction," *Composites Science and Technology*, Vol. 59, April 1999, pp. 749–758. doi:10.1016/S0266-3538(98)00117-1

[12] Standard Test Method for Shear Properties of Composite Materials by V-Notched Rail Shear Method, *ASTM Book of Standards*, Vol. 15.03, ASTM D7078/D7078M-05, American Society for Testing and Materials, West Conshohocken, PA, 2005.

[13] Raju, K. S., and Tomblin, J. S., "Damage Characteristics in Sandwich Panels Subjected to Static Indentation Using Spherical Indentors," AIAA Paper 2001-1189, 2001.

[14] Tomblin, J. S., and Barbero, E. J., "Statistical Microbuckling Propagation Model for Compression Strength Prediction of Fiber-Reinforced Composites," *Composite Materials: Testing and Design*, edited by S. J. Hooper, Vol. 13, American Society for Testing and Materials, ASTM STP 1242, 1997, pp. 151–167.